ISBN: 978-3-95450-196-0 doi:10.18429/JACoW-ECRIS2018-TUP11

THE FIRST MEASUREMENT OF PLASMA DENSITY BY MEANS OF AN INTERFERO-POLARIMETRIC SETUP IN A COMPACT ECR-PLASMA TRAP*

E. Naselli†[1], D. Mascali, G. Torrisi, G. Castro, L. Celona, S. Gammino, M. Mazzaglia, G. Sorbello[2], Istituto Nazionale di Fisica Nucleare, Laboratori Nazionali del Sud (INFN-LNS), 95123 Catania, Italy

[1]also at Department of Physics and Astronomy, University of Catania, Via Santa Sofia, 64, 95123 Catania, Italy

[2]also at Department of Electrical, Electronics and Computer Engineering (DIEEI), University of Catania, viale A. Doria, 6, 95125 Catania, Italy

Abstract

This paper presents the first measurement of plasma density by a K-band microwave polarimetric setup able to measure the magnetoplasma-induced Faraday rotation in a compact size plasma trap. The polarimeter, based on rotating waveguide OMTs (OrthoModeTransducers), has been proven to provide reliable measurements of the plasma density even in the unfavorable conditions $\lambda_p \sim L_p \sim L_c$ (being λ_p, L_p and L_c the probing signal wavelength, the plasma dimension and the plasma chamber length respectively) that complicates the measurements due to multi-patterns caused by reflections of the probing wave on the metallic walls of the plasma chamber. An analysis method has been developed on purpose in order to discriminate the polarization plane rotation due to magnetoplasma Faraday rotation only, excluding the effects of the cavity resonator. The measured density is consistent with the previous plasma density interferometric estimations. The developed method is a powerful tool for probing plasmas in very compact magnetic traps such as Electron Cyclotron Resonance Ion Sources and for in-plasma β-radionuclides' decay studies.

INTRODUCTION

For the development of future ECRIS dedicated and advanced plasma diagnostic tools will be crucial. It is particularly necessary to implement non-intrusive diagnostics for probing electron density and temperatures. Among the others, a special mention is worth by Optical Emission Spectroscopy (OES) [1,2] and X-rays spectroscopy (XRS) [3] which however are both able to measure "partial" densities only, i.e. the ones related to specific energy domains.

Interferometry and microwave polarimetry (i.e., taking profit by magnetoplasma induced Faraday Rotation) are able to probe to whole plasma electron population, regardless of energy contents. These techniques have been fruitfully applied already in large-scale fusion reactors [4] and – regarding the Faraday rotation especially – are a standard in astrophysical plasmas, where used for either magnetic field and/or stellar density measurements [5].

However, the implementation of both the techniques in compact plasma traps, such as ECRIS, is still a challenge: the main constrain consists in the small-size of the plasma chamber and of the plasma itself if compared with the probing wavelength. The following condition holds: $\lambda_p \sim L_p \sim L_c$, being λ_p, L_p and L_c the probing signal wavelength, the plasma dimension and the plasma chamber length respectively. That means, interference effects due to the metallic walls of the plasma chamber cannot be neglected, and in some conditions even prevail. A specific approach has been therefore proposed and implemented, and a new double-purpose tool named VESPRI has been constructed: it is a microwave interfero-polarimeter suitable for total electron density measurements in ECRIS plasmas. At least for the interferometry in compact devices, data are already published elsewhere [6].

Hereby we show the data coming from polarimetric measurements (preliminary dataset are already commented in the paper [7]) that have allowed the first line-integrated measurement of plasma density via Faraday-rotation in ECRISs.

EXPERIMENTAL SETUP

The measurement of the magnetoplasma induced rotation of the polarization plane in the VESPRI setup has been based on broadband waveguide OrthoModeTransducers (OMTs) system (see Fig. 1).

The turnstile junction OMTs enable the TE11 mode from the circular input port of the conical horn antennas to be split equally into the two single-mode rectangular waveguide outputs TE10 modes, thus obtaining a return loss better than 13 dB in the 18÷26.5 GHz band. One of the twos OMTs can rotate at ± 95°, with an angular precision of 0.05°, handling up to 100 W of microwave power (but the probing signal was below 100 mW due to the high sensitivity of the power probe). The OMTs were inserted along the plasma leg, upstream and downstream to the emitting/receiving antennas.

*Work has received funding from 5th Nat. Committee of INFN, under the grants VESPRI and PANDORA
† naselli@lns.infn.it

ISBN: 978-3-95450-196-0 doi:10.18429/JACoW-ECRIS2018-TUP11

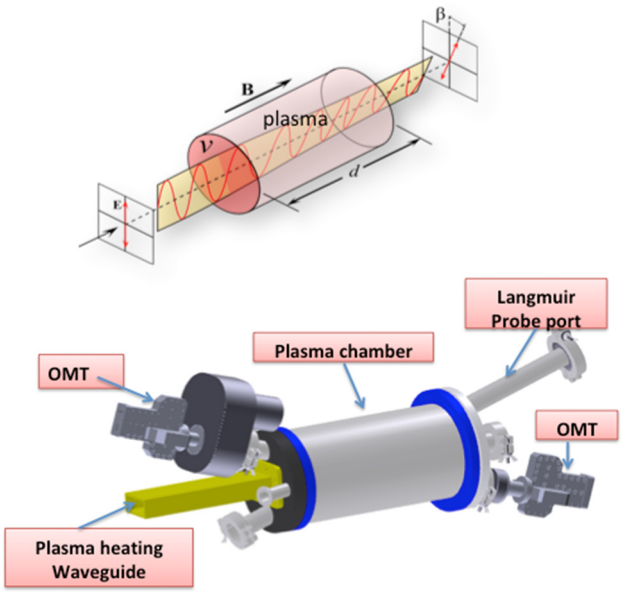

Figure 1: Up – simplified sketch of Faraday rotation induced by the magnetoplasma. Down – Drawing of the Orthomode transducers used as microwave-polarimeters connected to the plasma chamber. A Langmuir probe was simultaneously used to compare density data.

The angle of the rotating OMT is changed (via in-vacuum rotatable joint connection in circular waveguide standard) in order to minimize its received power on the Cross-polar port. In free-space and empty cavity case (i.e., if the cavity effects are negligible), the angle fulfilling cross-polarisation condition corresponds to $\theta = \theta_{min} = 90°$.

The plasma changes the cross-polarization condition such as $\theta_{min}{}^{p} = \theta_F + \theta_{min}$, due to the additional depolarization angle θ_F induced by the Faraday effect on the propagating wave.

UNDERLYING THEORY

The derived Faraday's angle can then correlated to magnetoplasma parameters through the well-known relation:

$$\vartheta_F = \frac{\omega}{c}\frac{1}{2}\left(\sqrt{1-\frac{\omega_p^2}{\omega(\omega-\omega_g)}}-\sqrt{1-\frac{\omega_p^2}{\omega(\omega+\omega_g)}}\right) = \frac{k_0'-k_0''}{2} \quad (1)$$

The pulsations appearing in Eq. (1) assume the usual meaning of pumping, gyro and plasma frequencies, while c is the speed of light.

The Faraday angle dependence on such pulsations can be highly simplified in case $\omega >> \omega_p$ and $\omega >> \omega_g$, assuming the famous form of the so-called "lambda-squared" law:

$$\vartheta_F = \frac{1}{2c}\left(\frac{\omega_p}{\omega}\right)^2 \omega_g = \frac{e^3\lambda_p^2 B_0 n_e}{8\pi^2 c^3 m_e^2 \varepsilon_0} \quad (2)$$

Equation (2) shows that once known B_0, i.e. the induction of the externally applied magnetostatic field, is possible to univocally derive the plasma density from a linearized fitting procedure θ_F vs. λ^2. Actually, for probing microwaves in the range 18÷30 GHz, that is the one of our setup, only the condition $\omega >> \omega_g$ applies, since the expected densities (order of 10^{12} cm^{-3}) violate the second assumption. Hence, Eq. (1) has been developed in series of ω/ω_p, truncating the series at the 4th term:

$$\vartheta_F = \frac{q_e^3}{2cm_e^2\varepsilon_0}\int_0^L\left(\frac{nB}{\omega^2}+\frac{q_e^2}{m_e\varepsilon_0}\frac{n^2B}{2\omega^4}+\frac{q_e^4}{m_e^2\varepsilon_0^2}\frac{n^3B}{4\omega^6}+\frac{q_e^6}{2cm_e^3\varepsilon_0^3}\frac{n^4B}{6\omega^8}\right)dx \quad (3)$$

The integral stands for the variation of n and B along the line of sight. In general, in ECRIS-like systems, B profile is well-known, while n(l) can be argued depending on the magnetic structure (flat-B field, Simple Mirror, B-minimum) with reasonable precision. Figure 2 shows how big is the difference between the Faraday's law and its approximation, at a density of $3\cdot10^{12}$ cm^{-3}.

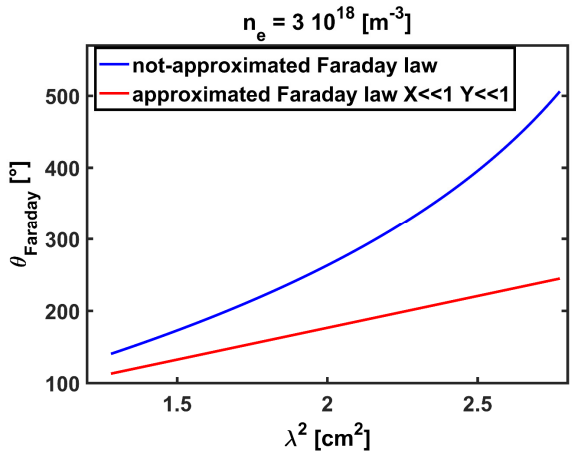

Figure 2: Calculated trends of the expected Faraday angles for approximated and not-approximated Faraday law as a function of λ^2.

DATA ANALYSIS STRATEGY

Due to the already mentioned cavity-induced effects, which superimpose to the straight signal going from the emitting to the receiving antenna, acquired data vs. frequency (or, equivalently, versus the wavelength) must be accurately depurated by spurious components. In particular, we want that the polarization measurements occur more

ISBN: 978-3-95450-196-0 doi:10.18429/JACoW-ECRIS2018-TUP11

or less as in free-space, where co and cross polarization conditions are well-known, following the Malus' law:

$$P=P_0\cos^2\vartheta \qquad (4)$$

The frequency scan proceeds from 18 to 26.5 GHz, at steps of 0.6 MHz, thus collecting more than 13000 single frequencies. An analysis routine has been implemented in order to scan the dataset, applying Eq. (4) in terms of statistical agreement to the linearized relation P vs. $\cos^2\vartheta$.

The filtering consists in eliminating only those frequencies which are dominated by cavity modes and do not fulfil Eq. (4) condition when varying the reciprocal orientation of OMTs. This filtering is practically applied via the statistical correlation parameter R. The higher is the request in terms of R (i.e., for R closer and closer to 1) the lower is the number of frequencies that can be selected. Typically, R parameters >0.99 were needed in order to obtain datasets with good "signal-over-noise" ratios.

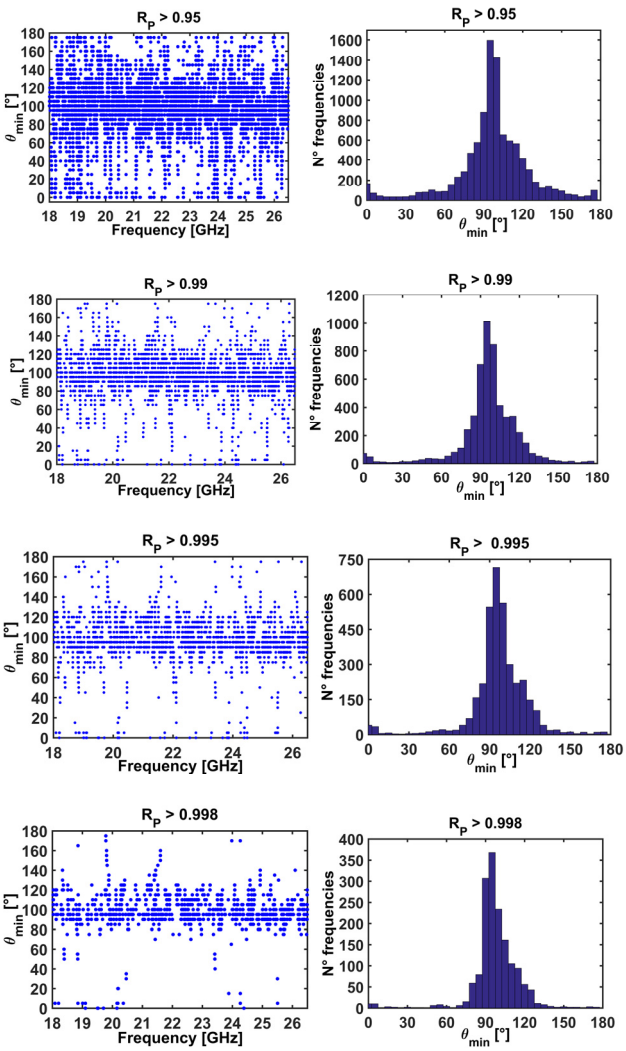

Figure 3: The sequence of plots (scatter and histograms types) represent the selected frequencies dataset at increasing "filtering strength", i.e. for R-parameters closer and closer to 1.

Figure 3 displays a sequence of in-cavity experimentally obtained data sets: the cross-polarization angle (here named θ_{min}) is measured along the whole frequency scan. Only the frequencies fulfilling Malus law are plotted, at increasing R-correlation parameter. The ideal case corresponding to free-space configuration is when the angle for minimum transmission (i.e., the cross-polar condition) is exactly equal to 90°. Cavity effects, introduce waves scattering then implying a broad distribution of angles for which the cross-polarization condition occurs.

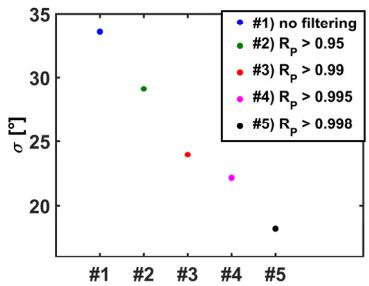

Figure 4: Standard deviation of the histograms in Fig. 3: at increasing R the angular dispersion drops.

The final number of frequencies was a compromise between accuracy of the filtering and statistical consistence of the dataset. From each histogram of Fig. 3 a relative standard deviation can be calculated, as shown in Fig. 4: it somehow relates to the data spread, hence with the accuracy by which the rotation angle can be measured.

EXPERIMENTAL BENCHMARKS IN EMPTY PLASMA CHAMBER

In order to verify that the device is able to distinguish among different polarization angles inside the resonant cavity, we implemented a benchmark setup based on a microwave-wire grid polarizer, according to the sketch of Fig. 5.

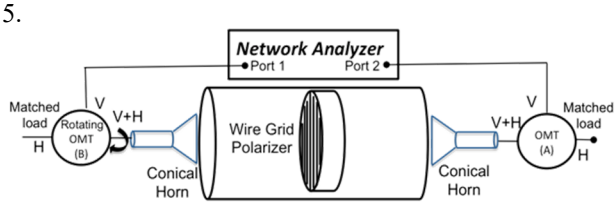

Figure 5: sketch of the experimental setup where a wire-grid microwave polarized has been placed inside the plasma chamber.

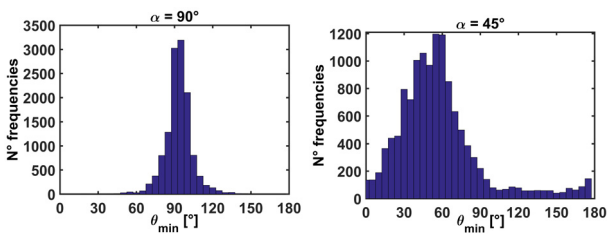

Figure 6: Histograms of minimum-angles in case of polarizer placed inside the plasma chamber, at two different angles. Data show that the device is able to detect a variation of the polarization axis.

ISBN: 978-3-95450-196-0 doi:10.18429/JACoW-ECRIS2018-TUP11

The polarizer was placed inside the plasma chamber, around the midplane. The polarizer almost completely fits inside the chamber diameter, and its polarization angle α was rotated at steps of 15°. For sake of brevity, here we present results for 45° and 90°. Figure 6 summarizes the results for these two angles. It is already clear that despite the broad data dispersion due to the in-cavity scattering, anyway the system is able to detect the different polarizer angle. A more quantitative analysis can be carried out.

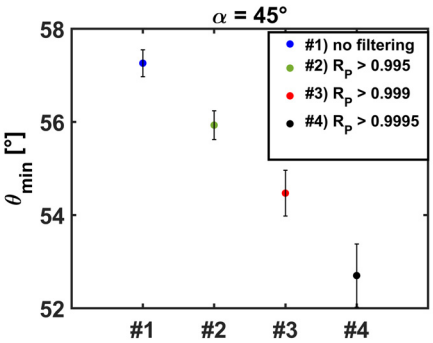

Figure 7: Estimation of θ_{min} in case of benchmark measurements with the microwave polarizer: data show that at increasing "filtering-strength" in terms of the R parameter, data tend to the expected value.

The results of the quantitative analysis are summarized in Fig. 7. The plot reports the average value of θ_{min} as coming out from four datasets obtained at different "filtering-strength", in terms of the correlation R parameter. The standard error is also plotted. It is clear that at increasing R the measured angle becomes closer and closer to the expectation angle $\alpha = 45°$.

These results demonstrate that the developed method is robust in determining any change in the polarization plane of the wave propagating inside a resonant cavity, with a relative error in the order of 10%.

The following step was therefore to measure polarization angle variation induced by the magnetoplasma.

IN-PLASMA MEASUREMENTS

After the benchmark measurements the VESPRI polarimeter has been used for the first time to detect magnetoplasma induced rotation of the probing wave polarization plane. The main results are illustrated in the three plots of Fig. 8.

Each points in Figs. 8a,b,c is the result of an average in θ_{min} obtained in a given Δf (or, equivalently, $\Delta\lambda$) bin. The bin size is a compromise between the minimal number of points needed for a good best-fit calculation, and the minimal amount of data in a given bin to have a significant estimation of the $<\theta_{min}>$ with its own error-bar. The three plots allow a direct comparison of what happens in three different situations:

(a) *free space*: the θ_{min} averages at 90° (standard cross polar configuration), and data have a very low fluctuation around the expectation value; the line corresponds to the attempted correlation to the 4th order truncated Faraday law (Eq. (3)), showing no correlation at all (the corresponding R parameter is 0.08).

(b) *empty cavity*: the θ_{min} averages again at 90° (standard cross polar configuration), but now data show wide fluctuations around the expectation value, due to the scattering introduced by the cavity; now the R correlating to Eq. (3) is -0.0094, again supporting uncorrelated hypothesis for vacuum propagation, despite the presence of the cavity;

(c) *In-plasma:* in this case, a N plasma has been excited at 1.5 10^{-4} mbar, using 130 W of microwave power. Now a trend of the θ_{min} vs. λ^2 is clearly evident. The correlation to the Faraday law is confirmed by the R parameter, being R=0.88. Considering the number of points in the best-fit procedure, tables for statistical consistency say this value provides a "very high" probability of dataset correlation to the given mathematical law.

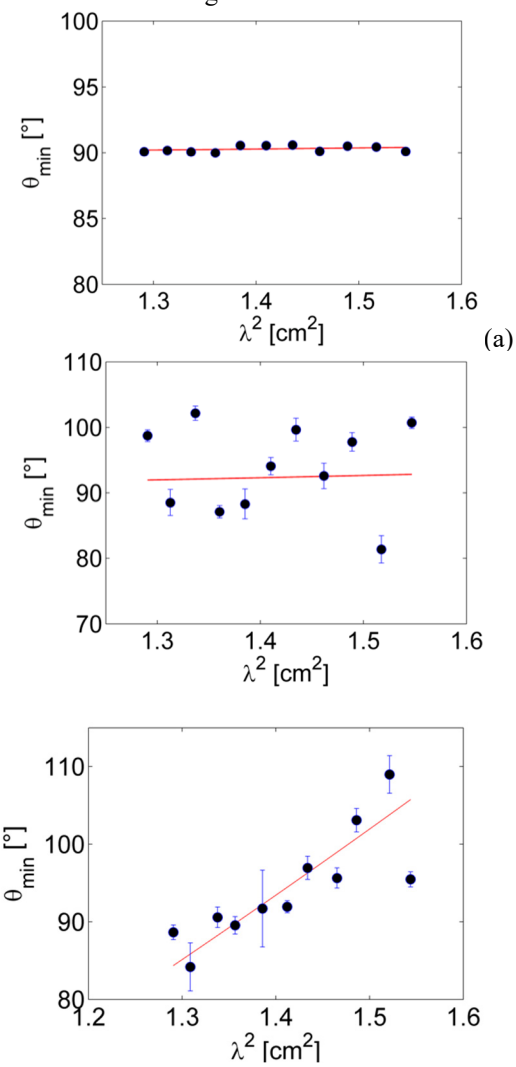

Figure 8: Sequence of plots regarding the θ_{min} vs. λ^2 when using the 4th term truncated Faraday law (Eq. (3)), in case of: (a) free-space measurements; (b) measurements in an empty plasma chamber; (c) measurements in presence of the magnetoplasma.

ISBN: 978-3-95450-196-0 doi:10.18429/JACoW-ECRIS2018-TUP11

Using Eq. (3) is therefore possible to extrapolate the value of the electron density as a free-parameter of the best fit procedure. The result is displayed in Fig. 9.

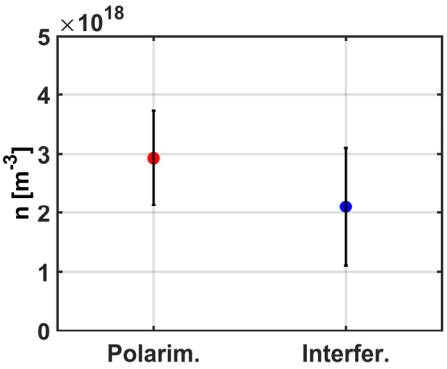

Figure 9: Estimation of the electron density from the best-fit procedure on the dataset of Fig. 8c, according to the equation 3. The result obtained by interferometric measurements [6] is also reported, for comparison.

The polarimetric measurement amounts to $(2.93\pm0.8)\cdot10^{18}$ m^{-3}, that is in good agreement with interferometric estimations $(2.1\pm1.0)\cdot10^{18}$ m^{-3}. The special analysis method has also permitted to reduce the relative errors. Langmuir probes measurements in identical physical conditions have been performed and give a density a factor 4 lower: possible explanations have been discussed in details in [6].

CONCLUSIONS

In this paper we have presented the first results concerning the Faraday-rotation measurements in compact plasma traps such as ECR Ion Sources. The developed analysis procedure has permitted to estimate the rotation angle of the probing wave polarization plane, then correlating it to the plasma density value, that can be estimated with a relative error of around 25%. The method opens new perspectives about non-intrusive plasma diagnostics with the goal to improve the tuning of existing machines and the design of the new ones.

REFERENCES

[1] G. Castro, M. Mazzaglia, D. Nicolosi, D. Mascali, R. Reitano, L. Celona, O. Leonardi, F. Leone, E.Naselli, L. Neri, G. Torrisi, S. Gammino and B. Zaniol, "Application of Optical Emission Spectroscopy to high current proton sources", (2018)

[2] Kronholm R, Kalvas T, Koivisto H, Tarvainen O. "Spectroscopic method to study low charge state ion and cold electron population in ECRIS plasma". , vol 89(4), p. 043506, (2018).

[3] D. Mascali, L. Celona, F. Maimone, J. Maeder, G. Castro, F.P. Romano, A. Musumarra, C. Altana, C. Caliri, G. Torrisi, L. Neri, S. Gammino, K. Tinschert, K. P. Spaedtke, J. Rossbach, R. Lang and G. Ciavola. "X-ray spectroscopy of warm and hot electron components in the CAPRICE source plasma at EIS testbench at GSI", vol. 85, p. 02A956, (2014)

[4] E. E. Scime, R. F. Boivin, J. L. Kline, and M. M. Balkey, .vol. 72, p. 1672 (2000)

[5] P.S. Ramkumar and A.A. Deshpande, "Determination of Linear Polarization and Faraday Rotation of Pulsar Signals from Spectral Intensity Modulation", , vol..20, pp. 37-50, (1999)

[6] D. Mascali, G. Torrisi, O. Leonardi, G. Sorbello, G. Cas-tro, L. G. Celona, R. Miracoli, R. Agnello, and S. Gammino, "The first measurement of plasma density in an ECRIS-like device by means of a frequency-sweep microwave interferometer", ω 095,109(2087) p.

[7] G. Torrisi, E. Naselli, D. Mascali, G. Castro, L. Celona, G. Sorbello, and S. Gammino, "A new interferometric/ polarimetric setup for plasma density measurements in com-pact microwave-based Ion Sources", λ α α αλα αλ , vol. 12, (2017)